

Theoretical studies on excited states of Ne_2^*

III. *Ab initio* spin-orbit studies at large separations for states dissociating to $\text{Ne} + \text{Ne}^*(3s)$

Friedrich Grein¹, Sigrid D. Peyerimhoff² and Rainer Klotz²

¹ Department of Chemistry, University of New Brunswick, Fredericton, New Brunswick, Canada E3B 6E2

² Lehrstuhl für Theoretische Chemie, Universität Bonn, Wegelerstrasse 12, D-5300 Bonn 1, Federal Republic of Germany

(Received May 13; revised and accepted July 31, 1987)

Previously reported potential curves for $0_g^-(^3P_0)$ and $0_u^-(^3P_0)$ of Ne_2 obtained from large-scale configuration-interaction calculations supplemented by semi-empirical spin-orbit calculations are compared with potential curves deduced from experimental studies by Beyer and Haberland. Although the agreement between curves is very good, the assignment of states is opposite. *Ab initio* spin-orbit coupling matrix elements were calculated based on large CI wavefunctions for states dissociating to $\text{Ne} + \text{Ne}^*(3s)$. It was found that they hardly change between 5 and $20a_0$. *Ab initio* spin-orbit corrected potential curves differ little from previous curves relying on the semiempirical treatment of spin-orbit coupling, and all former conclusions remain essentially unchanged.

Key words: Spin-orbit interaction — 3s states of Ne_2

1. Introduction

In part I of this series [1], potential energy curves without spin-orbit interaction were presented for excited states of Ne_2 dissociating to $\text{Ne} + \text{Ne}^*(3s, 3p, 4s)$. Extended basis sets were used with polarization and *s* and *p* diffuse functions

* Dedicated to Professor J. Koutecký on the occasion of his 65th birthday

on each atom. Large multireference configuration–interaction (CI) wavefunctions were employed, stretching the available programming and computer resources to the limit. The quantitative results are consistent with qualitative predictions for stable and repulsive states.

In the second part [2], spin–orbit corrections were added for states dissociating to $\text{Ne} + \text{Ne}^*(3s)$, using a semiempirical method due to Cohen and Schneider (CS) [3]. A constant spin–orbit coupling matrix element has been used for all distances, chosen such that it reproduces the experimentally observed spin–orbit splitting of $\text{Ne}(3s, ^1P)$ and $\text{Ne}(3s, ^3P)$. In order to achieve higher accuracy, the potential curves for the $3s$ states were recalculated with a lower threshold for configuration selection than before. An error limit of about 0.005 eV was estimated.

Comparing calculated minima and maxima with experimental results, it was found that dissociation energies of the “excimer” states $O_u^-(^3P_2)$, $1u(^3P_2)$ and $0_u^+(^3P_1)$ were too large by about 0.2 eV, whereas the very small potential barriers (~ 0.01 eV) were in some cases underestimated. The theoretical results were compared with spectroscopic findings for transitions originating in or leading to the ground state, and for absorption from the excimer states. For both situations, the agreement between theory and experiment was good, although a problem arose with respect to the stability of $1^{1,3}\Pi_g$, upper states postulated for the excimer absorption spectrum.

Not included in paper II was a comparison with experimental results obtained from atomic beam studies by Beyer and Haberland [4]. These authors found the ordering of $0_g^-(^3P_0)$ and $0_u^-(^3P_0)$ between 4 and $7a_0$ opposite to the ordering predicted by Cohen and Schneider [3].

Due to the fact that our ordering, using semiempirical spin–orbit corrections, agreed with that of CS, as will be shown in the following section, we decided to perform *ab initio* spin–orbit calculations for all states dissociating to $\text{Ne} + \text{Ne}^*(3s)$ at the larger distances of interest. Methods and results of *ab initio* spin–orbit calculations will be reported in this paper.

2. Comparison with semiempirical spin–orbit results

In Fig. 1, the calculated energies with semiempirical spin–orbit interaction (part II) of $0_g^-(^3P_0)$ and $0_u^-(^3P_0)$ are shown relative to the separated atoms $\text{Ne} + \text{Ne}^*(^3P_0)$, whose energy is placed at 0. Superimposed are the results derived by Beyer and Haberland [4] from measurements (solid curves). The results obtained by CS [3], also shown in Fig. 1, are at substantially higher energies. It is seen that at $7a_0$ our calculated energies are slightly lower than those of Beyer and Haberland, and that the calculated $0_g^-(^3P_0)$ potential starts deviating from the experimentally deduced curve below $5.5a_0$. Otherwise, the agreement of theoretical and experimentally deduced curves is excellent, except for one major point: the assignments 0_g^- and 0_u^- are opposite. Fig. 1 has been modified from Fig. 2 of [4]. The calculated values, obtained as energy differences from the data given in Table II of part II, are shown in Table 1.

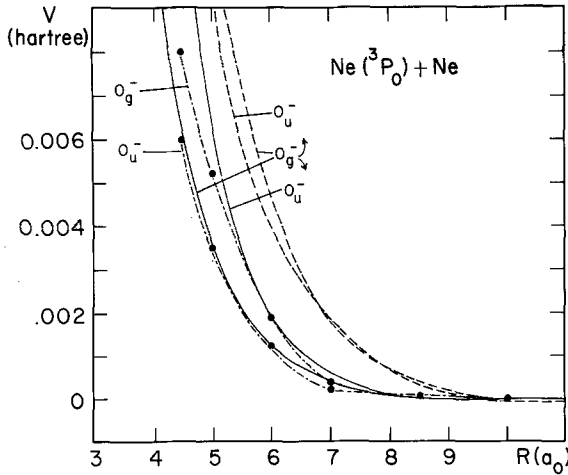


Fig. 1. Potential curves for $0_g^-(^3P_0)$ and $0_u^-(^3P_0)$ of Ne₂ deduced from atomic beam studies by Beyer and Haberland [4] (—), from theoretical studies by Cohen and Schneider [3] (---), and from this work (•- - - -•)

$0_g^-(^3P_0)$ is close to the former $1^3\Sigma_g^+$, and $0_u^-(^3P_0)$ is close to $1^3\Pi_u$. In support of the ordering of states as obtained theoretically, qualitative arguments, as outlined in section II of part I, suggest that at large distances $1^3\Sigma_g^+$ ($\sigma_g \rightarrow 3s$) should be steeper than $1^3\Pi_u$ ($\pi_u \rightarrow 3s$), since σ_g is more strongly bound than π_u . This implies that $1^3\Sigma_g^+$ (or $0_g^-(^3P_0)$) should be above $1^3\Pi_u$ (or $0_u^-(^3P_0)$) at large distances, as found theoretically. Both in the nonrelativistic and relativistic picture the two curves cross at about $4a_0$ (see Figs. 1 and 3 of part II). The reason for this crossing can be seen in the fact that $1^3\Sigma_g^+$ possesses a maximum at about $4a_0$, with a minimum at smaller R , whereas $1^3\Pi_u$ is strictly repulsive for all separations.

Due to the remaining discrepancy with experimentally deduced results of Beyer and Haberland [4], *ab initio* spin-orbit calculations were carried out for states of interest at large internuclear separations.

Table 1. Calculated potential energies using semi-empirical spin-orbit coupling. Energies in hartree relative to $\text{Ne} + \text{Ne}^*(^3P_0)$

$R(a_0)$	$E(0_g^-)$	$E(0_u^-)$
4.0	0.0118	0.0128
4.5	0.0080	0.0059
5.0	0.0052	0.0034
6.0	0.0018	0.0012
7.0	0.0003	0.0000 ^a
8.5	0.0001	0.0002 ^a
10.0	0	0

^a The estimated accuracy is 0.0002 a.u.

3. *Ab initio* spin-orbit calculations at large distances

Ab initio spin-orbit methods were developed and incorporated into the MRD-CI programming package by Buenker, Peyerimhoff and coworkers [5].

The CI wavefunctions used earlier in this work could not be used for spin-orbit calculations. Previously, the highest virtual orbitals $13\sigma_g$, $14\sigma_g$, $13\sigma_u$ and $14\sigma_u$ were “discarded”, which means excluded from excitations. Due to their potential significance for spin-orbit matrix elements, such measures are not feasible in *ab initio* spin-orbit calculations. Therefore, the CI orbital space had to be increased from 50 to 54MO's. The basis set was kept the same as before.

Calculations were performed with a selection threshold of $T = 2\mu h$ on the $2^1\Sigma_g^+$, $1^3\Sigma_g^+$, $1^1\Sigma_u^+$, $1^3\Sigma_u^+$, $1^1\Pi_g$, $1^3\Pi_g$, $1^1\Pi_u$ and $1^3\Pi_u$ states at 4, 5, 6, 7, 8 and $20a_0$. The number of configurations selected for diagonalization ranged from 9000 to over 15 000. All calculated energies are lower than before, due to the increased CI orbital space, but the qualitative appearance of the potential curves, as well as energy differences, are in close agreement with previous results. Overall, the long range minima and maxima are more pronounced, and some new ones appear that were not previously present. It is not clear at this moment whether such changes are due to the increased MO space or to the decreased accuracy (lower selection threshold). As before, $1^3\Sigma_g^+$ lies well above $1^3\Pi_u$.

Using the unabridged CI wavefunctions, spin-orbit elements were calculated as far as necessary for the $\Omega = 0$ states. They are given in Table 2. It is seen that between 5 and $20a_0$, all spin-orbit matrix elements (absolute) lie between 220.9 and 226.1 cm^{-1} , with hardly any distance variation. This fact supports the assumption of a constant (semiempirical) matrix element at large distances. In absolute terms, all matrix elements are smaller than the semiempirical value of 258.7 cm^{-1} used before, as given by Cohen and Schneider [3]. Between 5 and $4a_0$, two of the matrix elements experience a significant drop of about 45 cm^{-1} below the previously held range. Both matrix elements contain $1^3\Pi_g$.

The spin-orbit corrected energies were calculated by diagonalizing the following matrices:

For $\Omega = 0$:

$$\begin{bmatrix} E(^3\Pi) + \langle ^3\Pi^+ | ^3\Pi^+ \rangle & \langle ^3\Pi^+ | ^3\Sigma^+ \rangle & \langle ^3\Pi^+ | ^3\Pi^- \rangle & \langle ^3\Pi^+ | ^1\Sigma^+ \rangle \\ \langle ^3\Sigma^+ | ^3\Pi^+ \rangle & E(^3\Sigma) + \langle ^3\Sigma^+ | ^3\Sigma^+ \rangle & \langle ^3\Sigma^+ | ^3\Pi^- \rangle & \langle ^3\Sigma^+ | ^1\Sigma^+ \rangle \\ \langle ^3\Pi^- | ^3\Pi^+ \rangle & \langle ^3\Pi^- | ^3\Sigma^+ \rangle & E(^3\Pi) + \langle ^3\Pi^- | ^3\Pi^- \rangle & \langle ^3\Pi^- | ^1\Sigma^+ \rangle \\ \langle ^1\Sigma^+ | ^3\Pi^+ \rangle & \langle ^1\Sigma^+ | ^3\Sigma^+ \rangle & \langle ^1\Sigma^+ | ^3\Pi^- \rangle & E(^1\Sigma) + \langle ^1\Sigma^+ | ^1\Sigma^+ \rangle \end{bmatrix}.$$

For all matrix elements the operator is the spin-orbit Hamiltonian, as given by the Breit-Pauli formulation

$$H_{\text{SO}} = \frac{e^2 \hbar^2}{2m^2 c^2} \left[\sum_{i,\alpha} \frac{Z_\alpha}{r_{i\alpha}^3} (\mathbf{r}_{i\alpha} \times \mathbf{p}_i) \cdot \mathbf{s}_i + \sum_{i \neq j} (\nabla_i \mathbf{r}_{ij}^{-1} \times \mathbf{p}_i) \cdot (\mathbf{s}_i + 2\mathbf{s}_j) \right],$$

Table 2. *Ab initio* spin-orbit matrix elements in cm⁻¹ for low-lying excited states of Ne₂

<i>M</i> / <i>R</i> (a ₀)	4	5	6	7	8	20
$\langle 1^3\Pi_g L_y 2^1\Sigma_g^+ \rangle$	-175.71	-221.51	-223.63	-224.40	-224.67	-224.67
$\langle 1^3\Pi_g L_y 1^3\Sigma_g^+ \rangle$	178.76	221.86	224.35	225.10	225.47	225
$\langle 1^3\Pi_g L_z 1^3\Pi_g \rangle$	223.83	225.27	221.21	221.05	221.97	221.49
$\langle 1^3\Pi_u L_z 1^3\Pi_u \rangle$	219.36	224.71	220.92	220.93	221.60	221.40
$\langle 1^3\Pi_u L_y 1^3\Sigma_u^+ \rangle$	-224.00	-226.06	-225.67	-225.31	-225.37	-225.02
$\langle 1^3\Pi_u L_y 1^1\Sigma_u^+ \rangle$	-222.89	-224.00	-225.07	-224.65	-224.53	-224.47

where Z_α is the charge on nucleus α , the summations extend over all electrons and nuclei, and r_i , p_i , and s_i are the position, linear momentum, and spin vectors (operators) for electron i . It is understood that for the $\Omega = 0$ matrix, given above, and the following matrices for $\Omega = 1$ and 2, only the appropriate components of the wavefunctions are to be chosen. For example, for $\Omega = 0$, $\langle ^3\Pi^+ | ^3\Pi^- \rangle$ is $\langle ^3\Pi(M_L = 1, M_S = -1) | H_{SO} | ^3\Pi(M_L = -1, M_S = 1) \rangle$. In all cases, the matrices have to be solved separately for the g - and u -wavefunctions. For $\Omega = 1$:

$$\begin{bmatrix} E(^3\Pi) + \langle ^3\Pi | ^3\Pi \rangle & \langle ^3\Pi | ^3\Sigma^+ \rangle & \langle ^3\Pi | ^1\Pi \rangle \\ \langle ^3\Sigma^+ | ^3\Pi \rangle & E(^3\Sigma^+) + \langle ^3\Sigma^+ | ^3\Sigma^+ \rangle & \langle ^3\Sigma^+ | ^1\Pi \rangle \\ \langle ^1\Pi | ^3\Pi \rangle & \langle ^1\Pi | ^3\Sigma^+ \rangle & E(^1\Pi) + \langle ^1\Pi | ^1\Pi \rangle \end{bmatrix}.$$

For $\Omega = 2$:

$$E(^3\Pi) + \langle ^3\Pi | ^3\Pi \rangle.$$

Evaluating the various integrals by using group theoretical principles leads to the following matrices, expressed by the matrix elements as calculated and given in Table 2.

For $\Omega = 0$, example of g -wavefunction:

$$\begin{bmatrix} E(^3\Pi_g) + \langle ^3\Pi_g | ^3\Pi_g \rangle & -\langle ^3\Pi_g | ^3\Sigma_g \rangle & 0 & \langle ^3\Pi_g | ^1\Sigma_g^+ \rangle \\ -\langle ^3\Pi_g | ^3\Sigma_g^+ \rangle & E(^3\Sigma_g^+) & -\langle ^3\Pi_g | ^3\Sigma_g^+ \rangle & 0 \\ 0 & -\langle ^3\Pi_g | ^3\Sigma_g^+ \rangle & E(^3\Pi_g) + \langle ^3\Pi_g | ^3\Pi_g \rangle & -\langle ^3\Pi_g | ^1\Sigma_g^+ \rangle \\ \langle ^3\Pi_g | ^1\Sigma_g^+ \rangle & 0 & -\langle ^3\Pi_g | ^1\Sigma_g^+ \rangle & E(^1\Sigma_g^+) \end{bmatrix}.$$

Here, and in the following, the matrix elements correspond to the notation of Table 2. For example, $\langle ^3\Pi_g | ^3\Pi_g \rangle$ is now $\langle 1^3\Pi_g | L_z | 1^3\Pi_g \rangle$.

For $\Omega = 1$, example of g -wavefunction:

$$\begin{bmatrix} E(^3\Pi_g) & -\langle ^3\Pi_g | ^3\Sigma_g^+ \rangle & -\langle ^3\Pi_g | ^1\Pi_g \rangle \\ -\langle ^3\Pi_g | ^3\Sigma_g^+ \rangle & E(^3\Sigma_g^+) & \langle ^1\Pi_g | ^3\Sigma_g^+ \rangle \\ -\langle ^3\Pi_g | ^1\Pi_g \rangle & \langle ^1\Pi_g | ^3\Sigma_g^+ \rangle & E(^1\Pi_g) \end{bmatrix}.$$

Since the emphasis of this paper was placed on $\Omega = 0$ states in order to correlate with the results of Beyer and Haberland, all of the spin-orbit matrix elements required for $\Omega = 0$ were evaluated by *ab initio* methods. Several of the $\Omega = 1$ matrix elements, however, were not calculated explicitly. Therefore, $\langle ^3\Pi_g | ^1\Pi_g \rangle$

was replaced by $\langle {}^3\Pi_g | {}^3\Pi_g \rangle$ and $\langle {}^1\Pi_g | {}^3\Sigma_g^+ \rangle$ by $\langle {}^3\Pi_g | {}^3\Sigma_g^+ \rangle$. Equivalent substitutes were made for u -matrix elements. Since all calculated matrix elements had nearly constant values between 5 and $20a_0$, the same can be assumed for the missing ones. Finally, for $\Omega = 2$ and g -states $E_{\text{SO}} = E({}^3\Pi_g) - \langle {}^3\Pi_g | {}^3\Pi_g \rangle$.

In the given matrices, $E({}^3\Pi)$, for example, is the energy obtained for ${}^3\Pi$ before spin-orbit interaction. Since the previously obtained $T = 1\mu h$ energies (part II) led to smoother and more accurate potential curves, they were used instead of the $T = 2\mu h$ energies calculated here. For 8.5 and $10a_0$, the matrix elements calculated at 8 and $20a_0$, respectively, were used.

4. Results and discussion

The energies calculated with the inclusion of *ab initio* spin-orbit matrix elements are given in Table 3. They differ from those obtained by semiempirical methods usually by only 0.1 mh, and at most by 0.4 mh. The energies at $4a_0$ are hardly any more affected by the new matrix elements than energies at larger distances. The new potential curves differ so little from the ones given in part II, using semiempirical spin-orbit corrections, that the graphs are virtually indistinguishable.

For the same reason, energy differences from Table 3 for $0_g^-({}^3P_0)$ and $0_u^-({}^3P_0)$ relative to their energies at $10a_0$ differ from those given in Table 1 by no more than 0.2 mh. Therefore, the conclusions drawn earlier about the energetic ordering of $0_g^-({}^3P_0)$ and $0_u^-({}^3P_0)$ remain unchanged.

In paper II of this series, the theoretical results were compared with spectroscopic absorption and emission studies. Absorption from the van der Waals minimum

Table 3. Calculated energies of Ne_2 ,^a including spin-orbit interaction, for $\Omega = 0, 1$ and 2, obtained using *ab initio* spin-orbit matrix elements

$R(a_0)$	$0_g^+/0_u^+({}^3P_1)$	$0_g^-/0_u^-({}^3P_0)$	$0_g^+/0_u^+({}^3P_1)$	$0_g^-/0_u^-({}^3P_2)$
4	3736/3784	3794/3784	3867/4087	3868/4127
5	3796/3876	3860/3878	3898/3930	3902/3967
6	3841/3884	3895/3902	3914/3917	3924/3942
7	3865/3886	3911/3914	3926/3927	3941/3950
8.5	3873/3882	3913/3911	3926/3926	3945/3943
10	3879/3884	3914/3913	3929/3929	3945/3944
$R(a_0)$	$1_g/1_u({}^1P_1)$	$1_g/1_u({}^3P_1)$	$1_g/1_u({}^3P_2)$	$2_g/2_u({}^3P_2)$
4	3794/3731	3830/3796	3879/4127	3886/3805
5	3848/3828	3873/3892	3910/3966	3917/3901
6	3865/3855	3908/3917	3927/3941	3931/3928
7	3876/3870	3925/3929	3941/3949	3942/3942
8.5	3877/3873	3928/3926	3945/3943	3942/3941
10	3881/3879	3929/3928	3945/3944	3945/3944

^a The values given are $(-E - 256) \times 10^4$, with E in hartree

of the ground state to $1_u(^3P_2)$, $0_u^+(^3P_1)$ and $0_u^+(^1P_1)$ has been postulated [6]. The latter state $0_u^+(^1P_1)$ was calculated to have a shallow minimum between 5 and $8.5a_0$. The *ab initio* spin-orbit calculations reported here are not changing the results obtained earlier to any significant extent.

Energy differences calculated for transitions occurring at smaller distances, like the absorptions originating in the excimer states at about $3.25a_0$, however, are expected to undergo larger changes when *ab initio* spin-orbit matrix elements are introduced, in particular when higher excited states not previously considered are included.

Acknowledgements. This study was supported by a visiting professorship from the Deutsche Forschungsgemeinschaft for F.G., and an operating grant from the Natural Sciences and Engineering Research Council of Canada. We are grateful to Prof. H. Haberland (Freiburg) for his continued interest.

References

1. Grein F, Peyerimhoff SD, Buenker RJ (1985) J Chem Phys 82:353
2. Grein F, Peyerimhoff SD (1987) J Chem Phys, in press
3. Cohen JS, Schneider B (1974) J Chem Phys 61:3230; Schneider B, Cohen JS (1974) J Chem Phys 61:3240
4. Beyer W, Haberland H (1984) Phys Rev A 29:2280
5. See, for example, Klotz R, Marian CM, Peyerimhoff SD, Hess BA, Buenker RJ (1984) Chem Phys 89:223 and references therein
6. Tanaka Y, Yoshino K (1972) J Chem Phys 57:2964

Note added in proof. According to a recent notification by Beyer and Haberland, an incorrect sign in the scattering amplitude has been found, causing interchange of the *g/u* classification, but not changing the derived potential curves in any other way. Therefore, the assignment of $0_g^-(^3P_0)$ and $0_u^-(^3P_0)$, as found in this work, is in agreement with the revised assignment of Beyer and Haberland.